antibiotics

MDPI

Article

One Health, One Photosensitiser: Hydroxypropyl-γ-cyclodextrin–Curcumin-Based Photodynamic Inactivation Across Abiotic Surfaces, Food Matrices and a Porcine Skin Model

Elisabeth Fischer [1], Isabella Salihovic [1], Anabel Cenit [1], Andreas Kubin [2], Lionel Wightman [2], Linda Jernej [1,3,†] and Kristjan Plaetzer [1,*,†]

[1] Laboratory of Photodynamic Inactivation of Microorganisms, Department of Biosciences and Medical Biology, University of Salzburg, 5020 Salzburg, Austria
[2] PLANTA Naturstoffe Vertriebs GmbH, 1230 Vienna, Austria
[3] Department of Dermatology and Venereology, Medical Faculty, Johannes Kepler University Linz, 4020 Linz, Austria
* Correspondence: kristjan.plaetzer@plus.ac.at
† These authors contributed equally to this work.

Abstract

Background/Objectives: Curcumin is a food-grade (E100) photosensitiser with promising antimicrobial properties, but its applicability is limited due to low water-solubility. Complexation of curcumin with hydroxypropyl-γ-cyclodextrin (HP-γ-CD) overcomes this constraint and may facilitate using a single photosensitiser for Photodynamic Inactivation (PDI) of pathogens along the food-production chain and within a One Health framework. Methods: In this study, a novel method to complex HP-γ-CD and curcumin (abbreviated as CD-Cur) was developed and the compound was tested against *Escherichia coli*, *Salmonella enterica*, and *Candidozyma auris*, in liquid culture and in situ on abiotic surfaces, food matrices, and a porcine skin model. Results: Planktonic experiments demonstrated concentration-dependent PDI efficacy with photokilling exceeding the 3 $\log_{10}$ threshold for all tested organisms at CD-Cur concentrations between 10 and 50 µM, illuminated with 435 nm (50 J/cm^2) LED light, while dark and light toxicity remained below microbiologically relevant levels. CD-Cur induced high reductions of viable *E. coli* on food-contact plastic foil (3.35 $\log_{10}$, 100 µM, white light, 100 J/cm^2) and on abiotic surfaces (5.17–5.50 $\log_{10}$, 30 µM, 435 nm, 25 J/cm^2) with visible photobleaching of the photosensitiser after illumination. On salmon and pistachios, matrix-dependent effects were observed, but PDI still achieved practically relevant reductions (2.25–3.52 $\log_{10}$, 30 µM, 435 nm, 200 J/cm^2) of *S. enterica* without visible colour alteration of the food. In a porcine skin model, CD-Cur in a 1% hydroxyethyl cellulose hydrogel reduced *C. auris* contamination notably. The addition of 2 mM EDTA further enhanced antifungal effects, indicating that CD-Cur can also be applied in a medical context as topical application on porcine skin (2.41 $\log_{10}$, 500 µM, 435 nm, 75 J/cm^2). Conclusions: Together, these results show that a single, photodynamic system based on food-grade CD-Cur can provide broad antimicrobial efficacy across diverse matrices and pathogens in a One Health context.

Keywords: *Candidozyma auris*; *Escherichia coli*; food decontamination; One Health approach; *Salmonella* spp.; skin disinfection; surface disinfection

Check for updates

Academic Editor: Maria Fernanda N. N. Carvalho

Received: 22 September 2026
Revised: 15 October 2026
Accepted: 21 October 2026
Published: 23 October 2026

Copyright: © 2026 by the authors. Licensee MDPI, Basel, Switzerland. This article is an open access article distributed under the terms and conditions of the Creative Commons Attribution (CC BY) license.

1. Introduction

The One Health concept recognises the interconnectedness of human, animal, and environmental health and emphasises the need for integrated strategies to prevent and control infectious diseases [1]. Transmission of pathogens frequently occurs across these domains, with the food-production chain representing a critical interface [2,3]. Along this chain, microorganisms can spread via contaminated raw materials, processing environments, and food-contact surfaces, finally reaching consumers [4,5]. Unsafe food causes an estimated 866 million illnesses and 1.5 million deaths annually, 30% being children under five, although representing only 9% of the global population. Africa and Southeast Asia account for the heaviest burden, and the economic impact reaches USD 310 billion in productivity losses annually, underscoring the urgent need for stronger food safety measures and coordinated One Health approaches across human, animal, plant, and environmental domains [6]. Foodborne pathogens such as *Salmonella* spp., and *Escherichia coli* continue to pose a major global health burden, causing millions of infections and substantial economic losses each year [6,7]. Besides sole foodborne pathogens, the yeast *Candidozyma auris* (formerly *Candida auris*) is recognised as a textbook example of a One Health relevant pathogen, as it probably developed as an environmental saprotroph, can persist on various surfaces, such as food and skin matrices, and many strains are resistant to multiple fungicides [8–10]. A major contributor to the development of resistant pathogens is the extensive use of antimicrobial agents in livestock production and plant agriculture. Beyond therapeutic applications, antimicrobials are frequently used for prophylaxis and growth promotion, accelerating the emergence and dissemination of antimicrobial resistance [11,12]. Furthermore, many pathogens can persist for longer times on abiotic surfaces, which enhances tolerance to disinfectants and facilitates cross-contamination during food processing [13–15].

These challenges underscore the urgent need for alternative, multi-target strategies that are effective, safe, and less prone to resistance development. Photodynamic Inactivation (PDI) has emerged as a promising approach, relying on light-activated photosensitisers (PS) to generate reactive oxygen species (ROS), including singlet oxygen and free radicals [16]. Produced ROS induce microbial cell death through oxidative damage to multiple cellular targets such as membranes, proteins, and nucleic acids. Due to its multi-target approach, it significantly reduces the likelihood of resistance development towards PDI compared to conventional antimicrobials, while PDI can also eradicate (multi-)resistant pathogens [17–20].

In recent years, PDI has gained increasing attention for applications in food safety and surface decontamination. It has demonstrated broad-spectrum activity against bacteria, fungi, and viruses across diverse environments [21–25]. Importantly, PDI can be applied under mild conditions and leaves minimal chemical residues, making it particularly suitable for food-related applications. Among potential PS, the food-grade substance curcumin has attracted interest due to its photochemical properties [26–29]. Curcumin is a yellow-orange, natural compound from the diarylheptanoid class and has a food additive grade by the European Union (E100). It is primarily extracted from the roots and pods of turmeric plants of the genus Curcuma, which comprises approximately 120 species, including Indian and Javanese turmeric. Historically, curcumin has been utilised for over 5000 years as a culinary ingredient and traditional remedy. Chemically, it is designated as (1E,6E)-1,7-bis(4-hydroxγ-3-methoxyphenyl)-hepta-1,6-diene-3,5-dione (IUPAC) [30]. However, its application is limited by poor aqueous solubility, low stability, and rapid degradation under environmental conditions [29]. At room temperature and neutral pH its solubility ranges between 1 and 10 μg/mL. Its absorption and fluorescence emissions lie within the 450–600 nm range, relevant for biological assays, although these properties are highly matrix- and solvent-dependent [31]. Curcumin demonstrates antimicrobial,

antibacterial, and antifungal activity [32]. In photodynamic diagnostics and therapy, curcumin is under investigation as a PS. Although other PS such as 5-ALA are widely used for generating protoporphyrin IX in hollow organs [33], its instability and photodegradation limit clinical utility [34,35]. Curcumin has shown potential in oncology [36], oral biofilm treatment [37], and wound infection management [38,39], but its poor bioavailability and water insolubility remain significant challenges. Existing co-precipitates and suspensions do not meet clinical development standards. The development of true curcumin complexes, as described herein, represents a novel approach to unlocking its application potential.

Cyclodextrins, cyclic oligosaccharides capable of forming inclusion complexes with hydrophobic molecules, offer an effective strategy to overcome these limitations [40]. Complexation with cyclodextrins enhances curcumin's solubility, stability, and bioavailability, while protecting it from degradation. This modification improves its performance as a PS and enables more consistent photodynamic activity in aqueous environments [41,42]. Also, cyclodextrins are generally recognised as safe and β-cyclodextrin is approved as food additive in the European Union (E459), providing a clear regulatory and safety advantage for applications in food systems and related One Health contexts [43,44]. The approval for the here used γ-cyclodextrin is pending.

Based on this context, this study investigates a complex of curcumin and hydroxypropyl-γ-cyclodextrin (CD-Cur) as a versatile antimicrobial strategy across multiple relevant environments. We hypothesise that CD-Cur will allow for effective PDI of key One Health-relevant pathogens, including *Escherichia coli*, *Salmonella enterica*, and *Candidozyma auris*, in liquid culture, and in pathogen-related model systems such as on abiotic surfaces, in food matrices, and in a skin model. We further propose that CD-Cur's improved solubility, stability, and photobleaching profile will support reproducible photodynamic activity across all tested contexts, although the required PS concentration and light dose may vary by matrix. This study serves as a proof-of-concept of the antimicrobial efficacy of CD-Cur, including photochemical description of the substance.

2. Results

2.1. CD-Cur Complex Characteristics

The PS complex consisting of curcumin and hydroxypropyl-γ-cyclodextrin (CD-Cur) was characterised with respect to its spectral properties, photostability, curcumin quantification, and aqueous solubility. The absorption spectrum of CD-Cur in DPBS (7% (*w*/*w*)) showed the characteristic curcumin absorption band (Figure 1A). Compared with curcumin dissolved in DMSO (1.13 a.u., at max. 435 nm), the complex exhibited a lower absorbance and a slight blue-shift in the maximum (0.54 a.u., at max. 425 nm). Nevertheless, the absorption profile remained within the spectral range relevant for blue- or white-light-mediated PDI.

Exposure-dependent bleaching was evaluated by illumination of CD-Cur with blue light (435 nm) at different radiant exposures (Figure 1B). CD-Cur in DPBS reached half-life ($t50$, Equation (1)) of its initial absorbance after 32.06 J/cm^2, comparable to native curcumin ($t50$ = 39.72 J/cm^2). CD-Cur dissolved in 1% hydrogel HEC showed somewhat faster photobleaching ($t50$ = 25.54 J/cm^2). These findings demonstrate that curcumin retains its light-responsive behaviour after complexation and that its photochemical properties can be assessed in aqueous and formulation-relevant media.

Curcumin concentration in the CD-Cur complex was determined by high-performance liquid chromatography (HPLC) using an external curcumin calibration curve (Figure 1C). The calibration curve showed a linear relationship between curcumin concentration and chromatographic response over the investigated concentration range. The curcumin loading can be adjusted by varying the ratio of the starting components and may be controlled over

a range of approximately 0.1–30% (*w*/*w*). For microbial applications a weight percentage of 7% (*w*/*w*) was chosen.

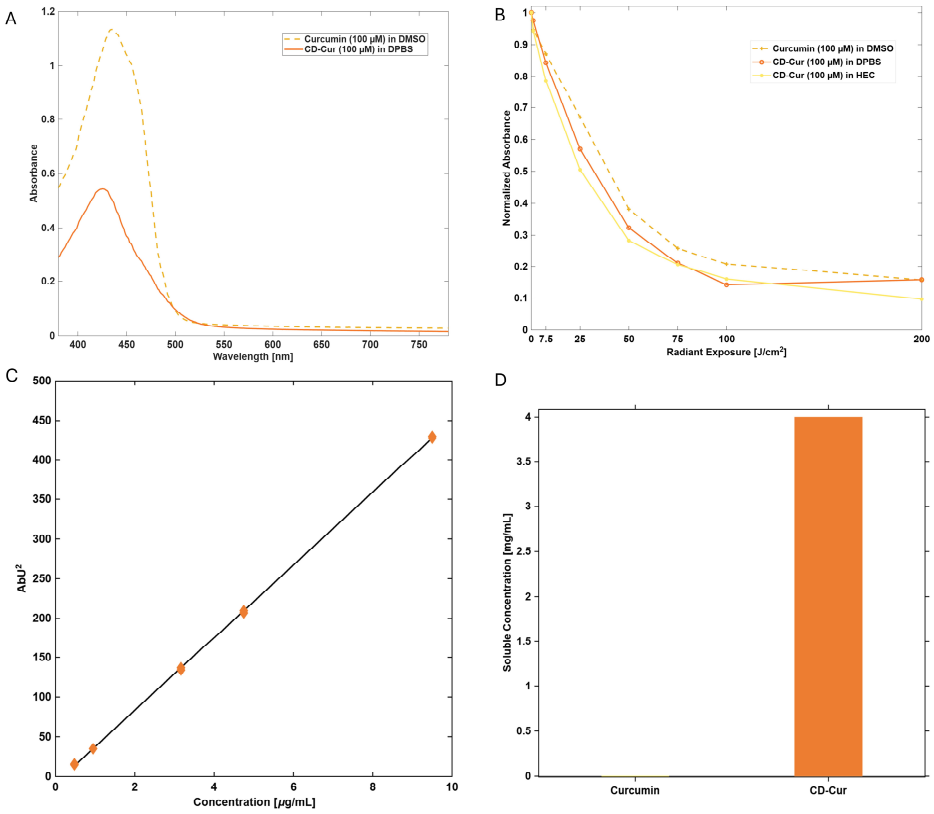


Figure 1. Characterisation of the curcumin–hydroxypropyl-γ-cyclodextrin (CD-Cur) photosensitiser complex. Absorption spectra of native curcumin at 100 µM in DMSO and CD-Cur at an equivalent curcumin concentration of 100 µM in DPBS (**A**). Exposure-dependent photobleaching of curcumin formulations with illumination at 435 nm and 24 mW/cm^2. Absorbance was normalised to the initial value (set to 1) and measured at increasing radiant exposure. Native curcumin (100 µM) dissolved in DMSO was compared to CD-Cur (100 µM curcumin) in DPBS and 1% hydrogel (HEC) (**B**). The regression relationship between curcumin concentration and HPLC response (Absorbance Units squared, AbU^2) was used to determine the curcumin content of CD-Cur (Regression y = 64x − 2, R^2 = 1). Curcumin loading can be adjusted by varying the ratio of the starting components and ranges from approximately 0.1 to 30% (*w*/*w*) (**C**). Native curcumin showed a solubility of approximately 0.0006 mg/mL, whereas CD-Cur showed a curcumin-related solubility exceeding 4 mg/mL (**D**).

Complexation markedly increased the apparent aqueous solubility of curcumin (Figure 1D). Free curcumin showed a solubility of approximately 0.0006 mg/mL in water. In contrast, CD-Cur displayed a curcumin-related solubility exceeding 4 mg/mL. Thus, complexation increased the apparent aqueous solubility by more than three orders of magnitude, enabling the preparation of substantially higher curcumin concentrations in aqueous media.

2.2. Photodynamic Inactivation on Planktonic Cultures

Planktonic culture experiments using CD-Cur and 435 nm LED light were performed with four different pathogens relevant within the One Health framework. A concentration-dependent increase in relative inactivation was observed for all tested microorganisms.

In the non-pathogenic *E. coli* K-12 strain, relative inactivation increased from 2.95 $\log_{10}$ steps at 10 µM CD-Cur to 5.38 $\log_{10}$ steps at 30 µM, which was the maximum. At higher concentrations, inactivation was 4.98 $\log_{10}$ steps at 40 µM and 3.82 $\log_{10}$ steps at 100 µM

(Figure 2A, 435 nm, 50 J/cm^2; Table S1). The 100 µM dark control showed minor relative inactivation of 0.32 $\log_{10}$ steps, comparable to the light-only control (0.59 $\log_{10}$ steps).

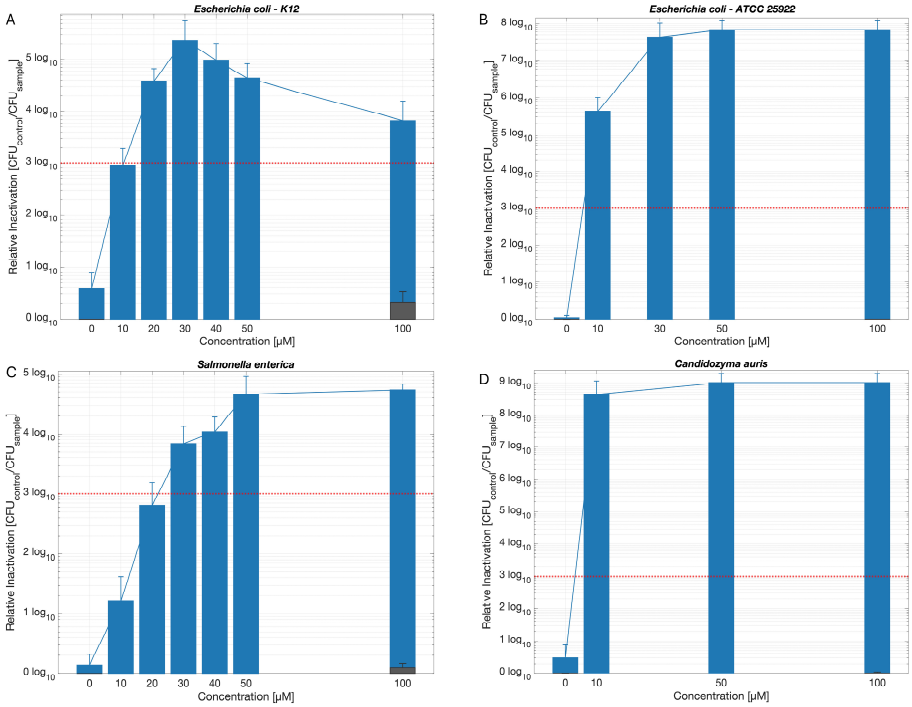


Figure 2. Mean relative inactivation of *Escherichia coli* K-12 (**A**), *Escherichia coli* ATCC 25922 (**B**), *Salmonella enterica* (**C**), and *Candidozyma auris* (**D**) after PDI treatment with increasing concentrations of CD-Cur and illumination at 435 nm LED light at 50 J/cm^2 for bacteria (**A**–**C**), and 7.5 J/cm^2 for *C. auris* (**D**). Given is the relative inactivation expressed as $\log_{10}$ ($CFU_{control}/CFU_{sample}$). Average CFU/mL of controls, serving as limit of detection: *E. coli* K12: 5.55×10^7, *E. coli* ATCC 25922: 1.17×10^8, *S. enterica:* 3.28×10^7, *C. auris:* 1.01×10^9. Grey bars at 100 µM indicate dark controls treated at respective CD-Cur concentration but restricted from light. The red dashed line indicates the threshold corresponding to a 3 $\log_{10}$ reduction. Biological replicates: $n \geq 3$. Error bars indicate standard deviation of relative inactivation of three replicates.

Pathogenic *E. coli* ATCC 25922 underwent enhanced photoinactivation at 10 µM CD-Cur, with a reduction of 5.63 $\log_{10}$ steps, while maximum inactivation was reached at 100 µM (7.84 $\log_{10}$ steps). The 100 µM dark control and light-only control showed no relevant inactivation (Figure 2B, 435 nm, 50 J/cm^2; Table S1).

The food-relevant pathogen *S. enterica* induced a progressive increase in photoinactivation with increasing CD-Cur concentration. Relative inactivation reached 4.66 $\log_{10}$ steps at 50 µM, and peaked at 4.73 $\log_{10}$ steps at 100 µM. The 3 $\log_{10}$ threshold was exceeded from 30 µM upward (Figure 2C, 435 nm, 50 J/cm^2; Table S1). The 100 µM dark control showed no notable photoinactivation (0.10 $\log_{10}$). Blue light alone reached an inactivation of 1.21 $\log_{10}$. Increasing the incubation time of the *S. enterica* culture in CD-Cur before illumination (DLI from 0 min to 15 min) decreased PDI efficiency by one $\log_{10}$ (Figure S2; Table S1).

Candidozyma auris demonstrated the highest overall susceptibility to CD-Cur-based PDI. Relative inactivation was 9.00 $\log_{10}$ steps at both 50 and 100 µM of CD-Cur, reaching the detection limit of the assay, even at a more-than-six-times lower irradiance compared to the bacterial experiments (Figure 2D, 435 nm, 7.5 J/cm^2; Table S1). The 100 µM dark control showed no inactivation. All planktonic culture results are summarised in Table S1.

2.3. Photodynamic Inactivation of Escherichia coli K12 on Plastic Foil

Photodynamic decontamination of *E. coli* K-12 from a food-packaging plastic foil coated with CD-Cur resulted in a 3.35 $\log_{10}$ reduction at 100 µM, thereby surpassing the 99.9% reduction criterion (Figure 3A, white light, 100 J/cm^2; Table S2). The light-only control (0 µM) showed 0.72 $\log_{10}$ steps of inactivation. At 30 and 50 µM, relative inactivation did not exceed the 3 $\log_{10}$ threshold (1.47 and 0.96 $\log_{10}$ steps, respectively). Although the overall response was less pronounced than in the liquid-suspension experiments, the data indicate that the treatment retained antimicrobial activity on the plastic surface and that higher compound concentrations enhanced efficacy. Representative images of the plastic foil before irradiation and after white-light exposure illustrate the experimental set-up and indicate bleaching of CD-Cur on the foil after illumination (Figure 3B). Results are summarised in Table S2.

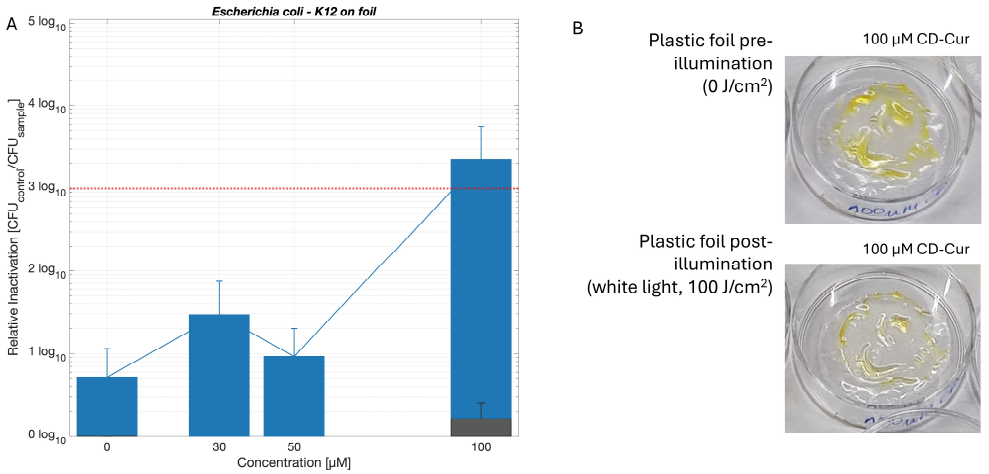


Figure 3. Decontamination of *Escherichia coli* K-12 on plastic foil. Relative inactivation after PDI treatment with increasing concentrations of CD-Cur and illuminated with a white-light lamp at 100 J/cm^2 expressed as $\log_{10}$ ($CFU_{control}/CFU_{sample}$). Average CFU/mL of control serving as limit of detection: 3.25 × 10^6. The grey bar at 100 µM represents the dark control at respective CD-Cur concentration but restricted from light. The red dashed line indicates the threshold corresponding to a 3 $\log_{10}$ reduction (**A**). Biological replicates: $n \geq 3$ Error bars indicate standard deviation of relative inactivation of three replicates. The right panel shows representative sample images of plastic foil before irradiation (0 J/cm^2) and after white-light illumination (100 J/cm^2) (**B**).

2.4. Photodynamic Inactivation of Escherichia coli on Abiotic Surfaces

Photodynamic disinfection of pathogenic *E. coli* ATCC 25922 using CD-Cur and blue light (435 nm, 25 J/cm^2) was tested on the surfaces of three different materials. The light intensity was selected based on previous experiments evaluating the bactericidal effect of blue light alone (Table S3). For all surfaces, CD-Cur at 30 µM induced a relative inactivation exceeding 5 $\log_{10}$ steps (ceramics: 5.17, metal: 5.22 and plastic: 5.50 $\log_{10}$ steps). However, on the ceramics surface, blue light alone (0 µM) also resulted in a reduction exceeding 4.57 $\log_{10}$ steps, indicating high light sensitivity of the pathogen on this white, smooth surface (Figure 4A; Table S4). Light toxicity did not exceed the 3 $\log_{10}$ threshold on plastic and metal surfaces. On the metal surface, the dark toxicity of 100 µM CD-Cur was 4.25 $\log_{10}$ steps, indicating a bactericidal effect of the PS alone (Figure 4C; Table S4). On all tested surfaces, the combination of PS and light increased the antimicrobial effect compared with each component alone. Comparable to the plastic foil, CD-Cur visibly bleached after illumination on the surfaces (Figure 4D). A summary of all results is given in Table S4.

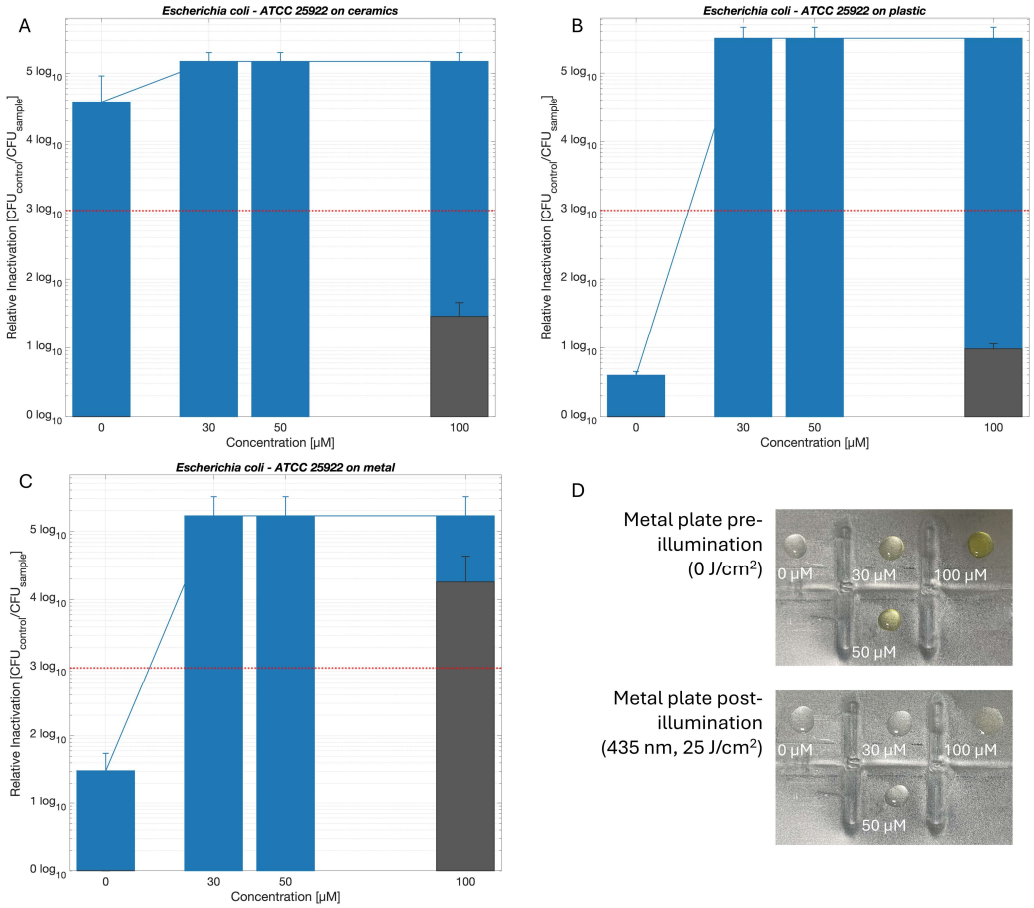


Figure 4. Surface disinfection of pathogenic *Escherichia coli* ATCC 25922 from ceramics (**A**), plastic (**B**), and metal (**C**) plates. Samples were disinfected by PDI using increasing concentrations of CD-Cur and were illuminated with 435 nm LED light at 25 J/cm^2. Given is the relative inactivation expressed as $\log_{10}$ (CFU$_{control}$/CFU$_{sample}$). Average CFU/mL of controls, serving as limit of detection: ceramics: 1.48×10^5, plastic: 3.19×10^5 and metal: 1.69×10^5). Grey bars at 100 µM indicate dark controls treated at respective CD-Cur concentration but restricted from light. The red dashed line indicates the threshold corresponding to a 3 $\log_{10}$ reduction. Biological replicates: $n \geq 3$ Error bars indicate standard deviation of relative inactivation of three replicates. Sample images before and after illumination of CD-Cur drops on the metal surface indicate a bleaching of the PS on the surface (**D**).

2.5. Photodynamic Inactivation of Salmonella enterica on Foodstuff

Blue light (435 nm, 200 J/cm^2) alone reduced *S. enterica* on all tested food matrices, and the addition of CD-Cur enhanced the efficiency. Using a lower radiant exposure of 100 J/cm^2 decreased light toxicity toward *S. enterica*, but also reduced photodynamic efficiency (Figure S3). To exclude antimicrobial effects caused by heating of the foodstuffs, the temperatures of pistachio and salmon samples were measured during illumination every 30 min. During exposure to the 435 nm LED array from 0 to 205 min, corresponding to a maximum radiant exposure of 300 J/cm^2, the temperature of pistachios increased from 22.25 °C to 32.85 °C, and that of salmon skin samples from 21.95 °C to 27.80 °C (Table S5). Temperature-dependent antimicrobial effects can therefore be excluded.

Photoinactivation varied on salmon skin samples depending on the colour of the skin. On light-skinned salmon, relative inactivation increased with increasing PS concentration, reaching a maximum of 2.91 $\log_{10}$ steps at 50 µM. Doubling the concentration to 100 µM decreased the photoinactivation to 1.56 $\log_{10}$ steps (Figure 5A; Table S6). On dark-skinned salmon, generally lower inactivation was achieved overall, with a maximum reduction of 2.25 $\log_{10}$ steps at 30 µM CD-Cur. Likewise, increasing the concentration to 100 µM did

not further improve efficacy (1.80 $\log_{10}$ steps) (Figure 5B; Table S6). In contrast, treatment of pistachios resulted in consistently high antimicrobial activity, with relative inactivation of 3.52 $\log_{10}$ steps at 30 µM, 3.18 $\log_{10}$ at 50 µM, and 3.23 $\log_{10}$ at 100 µM (Figure 5C; Table S6). Representative images of pistachios before and after illumination demonstrated no visible colour change after PDI treatment (Figure 5D). Results are summarised in Table S6.

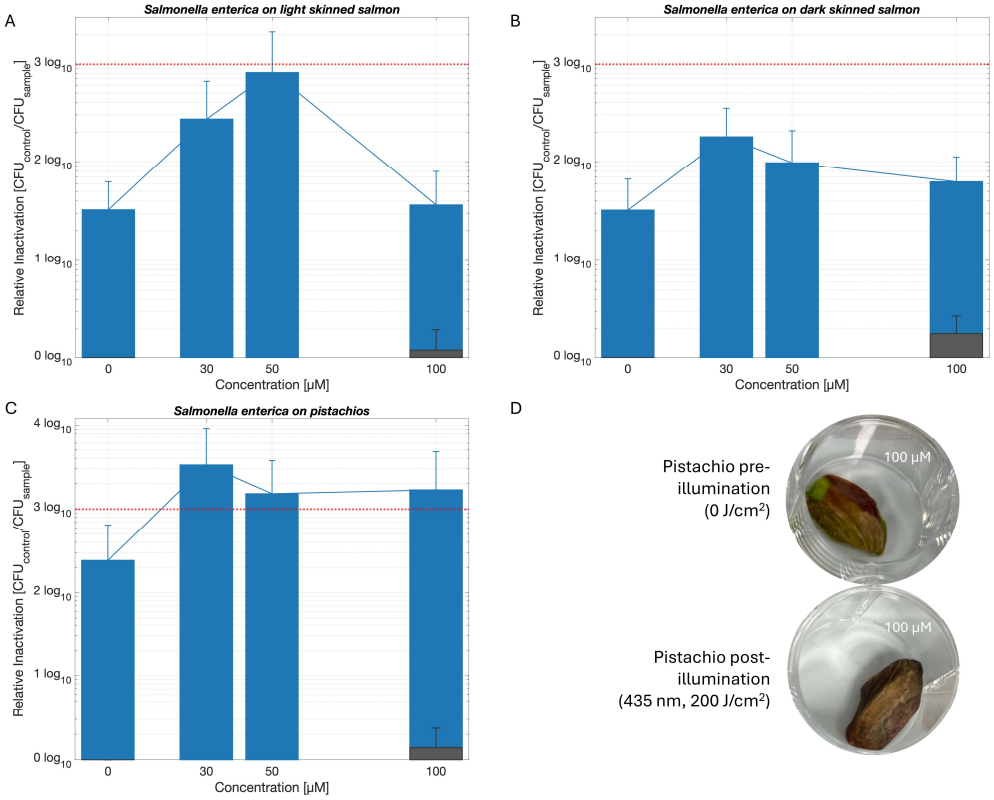


Figure 5. *Salmonella enterica* decontamination on light skinned salmon (**A**), dark skinned salmon (**B**), and pistachios (**C**). Samples were treated using increasing concentrations of CD-Cur and were illuminated with 435 nm LED light at 200 J/cm^2. Given is the relative inactivation expressed as $\log_{10}$ ($CFU_{control}/CFU_{sample}$). Average CFU/mL of controls, serving as limit of detection: light skinned salmon: 2.09 × 10^6, dark skinned salmon: 3.40 × 10^6, pistachios: 3.15 × 10^6. Grey bars at 100 µM indicate dark controls treated at respective CD-Cur concentration but restricted from light. The red dashed line indicates the threshold corresponding to a 3 $\log_{10}$ reduction. Biological replicates: $n \geq 3$ Error bars indicate standard deviation of relative inactivation of three replicates. Sample images before and after illumination of CD-Cur drops on pistachios indicate that there is no colour alteration post-PDI (**D**).

2.6. Photodynamic Inactivation of Candidozyma auris on a Porcine Skin Model

Preliminary experiments indicated that topical application of CD-Cur alone did not induce a relevant antimicrobial effect (values in Table S7). Therefore, CD-Cur and all controls were prepared in a 1% HEC hydrogel for skin applications. Illumination with CD-Cur in 1% HEC produced a concentration-dependent reduction in yeast, peaking at 2.00 $\log_{10}$ steps at 500 µM. Combining 2 mM EDTA with 500 µM CD-Cur somewhat enhanced the photoantifungal effect, resulting in 2.41 $\log_{10}$ steps of relative inactivation. In the absence of illumination (dark controls), no relevant reduction in the number of yeast cells was observed (Figure 6A, 435 nm, 75 J/cm^2; Table S8). Representative photographs of the porcine skin samples before and after illumination indicated photobleaching of CD-Cur after light exposure (Figure 6B). An overview of these results is given in Table S8.

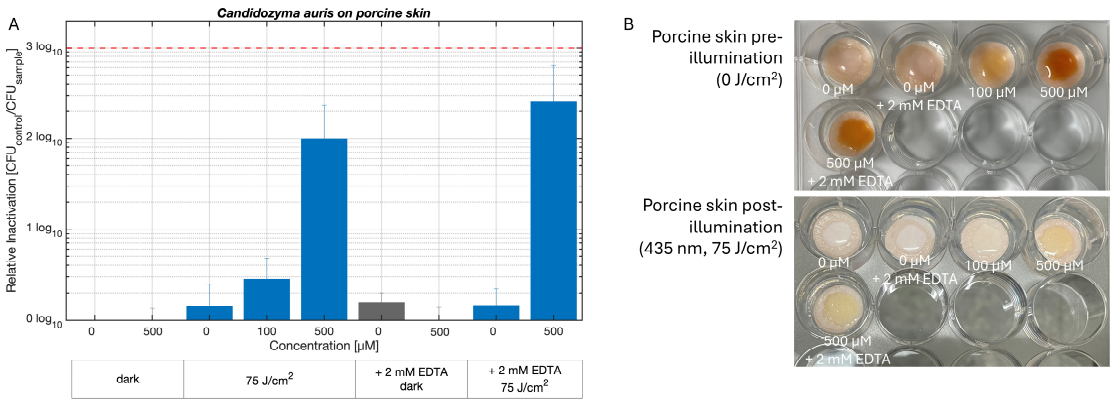


Figure 6. Disinfection of *Candidozyma auris* on porcine skin. Samples were treated with increasing concentrations of CD-Cur in 1% HEC and were illuminated with 435 nm LED light at 75 J/cm^2. Additional samples show results upon addition of 2mM EDTA. Given is the relative expressed as $\log_{10}$ ($CFU_{control}/CFU_{sample}$). Average CFU/mL in control, serving as limit of detection: 1.29×10^6. Grey bars indicate dark controls treated at respective CD-Cur concentration but restricted from light. The red dashed line marks the threshold corresponding to a 3 $\log_{10}$ reduction. Biological replicates: $n \geq 3$ Error bars indicate standard deviation of relative inactivation of three replicates. (**A**). Sample images of porcine skin samples treated with CD-Cur before and after illumination visualising bleaching of the PS (**B**).

An overview of all microbial assays is given in Table 1, presenting either the lowest concentration of CD-Cur that overcame the 3 $\log_{10}$ step criteria or achieved highest inactivation. Effective CD-Cur concentrations ranged from 10 µM to 500 µM, depending on the tested matrix. Most samples were illuminated with visible blue light (435 nm) at radiant exposures varying between 7.5 and 200 J/cm^2. These results indicate that CD-Cur has a broad potential application range, provided that the PDI parameters are adjusted appropriately.

Table 1. Overview of Photodynamic Inactivation of different One Health relevant pathogens in different matrices using CD-Cur in indicated concentrations, illuminated using a 435 nm LED array, if not indicated differently. The average inactivation ($\log_{10}$ reductions) is given for the lowest concentration that exceeds a 99.9% reduction in pathogen or the highest inactivation found in this study.

Matrix	Pathogen	CD-Cur Concentration [µM]	Radiant Exposure [J/cm^2]	Inactivation [$\log_{10}$ Reduction]
Liquid culture	*Escherichia coli*—K12	20	50	4.58
	Escherichia coli—ATCC25922	10	50	5.63
	Salmonella enterica	30	50	3.83
	Candidozyma auris	10	7.5	8.62
Plastic foil (food wrapping)	*Escherichia coli*—K12	100	100 *	3.35
Ceramics (plate)	*Escherichia coli*—ATCC25922	30	25	5.17
Plastic (acrylic)	*Escherichia coli*—ATCC25922	30	25	5.50
Metal (stainless steel)	*Escherichia coli*—ATCC25922	30	25	5.22
Dark skinned salmon	*Salmonella enterica*	30	200	2.25

Table 1. *Cont.*

Matrix	Pathogen	CD-Cur Concentration [μM]	Radiant Exposure [J/cm^2]	Inactivation [log$_{10}$ Reduction]
Light skinned salmon	*Salmonella enterica*	50	200	2.92
Pistachios	*Salmonella enterica*	30	200	3.52
Porcine skin	*Candidozyma auris*	500 (in 1% HEC)	75	2.00
Porcine skin	*Candidozyma auris*	500 (in 1% HEC) + 2 mM EDTA	75	2.41

* illuminated with a broad-spectrum white light.

3. Discussion

The present study introduces a novel, highly water-soluble curcumin–hydroxypropyl-γ-cyclodextrin complex (CD-Cur), with photophysical properties comparable to native curcumin (Figure 1). The resulting aqueous solution may be used as such or incorporated into pharmaceutical formulations. CD-Cur may therefore provide an aqueous formulation suitable for applications in which a clear, substantially particle-free formulation of a curcuminoid is required.

The advantage of using curcumin, extracted from the root *Curcuma longa,* in PDI lies in its food-grade nature, high consumer acceptance and availability in large quantities [45,46]. The photodynamic efficiency of curcumin is high, also against biofilms; however, it is limited to the disinfection of Gram-positive bacteria, due to its overall neutral charge [47,48]. Additionally, the delivery of lipophilic curcumin to physiological relevant tissue is a challenge that can be tackled by encapsulation or formulation of the substance. As alternative to these approaches, curcumin can also be chemically modified to have cationic moieties, which increase its water-solubility and photoefficiency against Gram-negative bacteria [49]. Yet, PDI of *E. coli* using cationic curcumin derivatives was less efficient compared to Gram-positive bacteria [27]. Another approach is the encapsulation into nanoparticles, thereby increasing the delivery potential of curcumin to active sites [50]. This approach is especially interesting for facilitating wound sterilisation [51]. However, neither the creation of chemically modified curcumin nor the encapsulation into nanoparticles preserves the most special characteristic of curcumin as a PS: its food-grade status. The complexation of curcumin with food-grade additives, such as polyvinylpyrrolidone could maintain this property, but was shown to have little to no efficacy against Gram-negative bacteria [29,52]. Increased photoinactivation efficiency towards Gram-negatives is given, if curcumin is complexed with cyclodextrins [53]. Gamma-cyclodextrin was simulated to act as drug carrier complex functioning as a shuttle for active compounds into lipid bilayers [54]. Complexing curcumin with cyclodextrin does not diminish ROS production from curcumin and can cause bacterial deformation and cell structure damage, as well as damaging microbial DNA and proteins [55].

Here we provide proof-of-concept that CD-Cur can achieve broad antimicrobial activity across several One Health-relevant pathogens and matrices. In planktonic cultures, CD-Cur activated by visible blue light (435 nm) at relatively low concentrations ($\leq$50 μM) and irradiance ($\leq$50 J/cm^2) achieved photoinactivation of non-pathogenic and pathogenic *E. coli*, *S. enterica* and *C. auris*, with log$_{10}$ reductions that consistently surpassed the commonly accepted 3 log$_{10}$ threshold, a descriptive value for antimicrobial efficacy [56] (Figure 2). Light-only and dark controls in liquid experiments confirmed that the observed effects were primarily driven by a photodynamic effect rather than toxicity to blue light or the CD-Cur formulation. These findings support the claim that curcumin complexed with cyclodextrin is a robust PS for antimicrobial use against food-relevant Gram-negative bacteria and the human pathogenic yeast *C. auris* [53].

Our results show that photodynamic efficacy is strongly influenced by the surrounding matrix. Whereas planktonic cultures were readily inactivated, solid surfaces and food matrices introduced additional restraints that likely affected light penetration, PS distribution, and microbial accessibility, resulting in high standard deviations among replicates. On plastic foil (Figure 3A), ceramics, plastic plates and metal (Figure 4A–C), high $\log_{10}$ reductions in *E. coli* were achieved, although pronounced light toxicity on white ceramics and notable dark toxicity at high PS concentrations on metal highlight that surface properties relativise the effect. Nevertheless, across all surface types, the combination of CD-Cur and visible blue light outperformed light or PS alone. In food matrices, the performance of the CD-Cur system was further challenged by the structural and compositional complexity of salmon skin and pistachios. For *S. enterica* on salmon, differences in skin colour were associated with varying PDI efficiency, with light-coloured samples allowing for higher $\log_{10}$ reductions (Figure 5A) and darker samples (Figure 5B) generally showing lower overall inactivation. This pattern is consistent with shielding effects by pigments, fats and proteins, which can attenuate light penetration or reduce effective PS availability at the microbial target sites [25,57]. In contrast, pistachios supported consistently high PDI efficacy (at $\geq$30 μM), exceeding a 99.9% reduction (Figure 5C). These results are encouraging for applications of CD-Cur in food-processing environments, where food-contact surfaces and equipment contribute substantially to cross-contamination along the food chain. However, practical use will require testing of sensory effects such as colour, odour, and texture. Although no visible discolouration was observed here, these model experiments do not yet reflect full industrial conditions. The existing literature indicates that cellulose films of curcumin complexed with cyclodextrin for food-packaging could inactivate pathogens on salmon and pork [58,59]. Our findings confirm this possible application across the food-production chain.

Extending the CD-Cur system to a porcine skin model inoculated with *C. auris* introduced a healthcare-relevant application within the One Health concept (Figure 6). CD-Cur in aqueous solution did not achieve a significant level of yeast photoinactivation. But when delivered in a hydroxyethyl cellulose hydrogel, >99% photoinactivation was induced. Moreover, the addition of 2 mM EDTA, which increases cell wall permeability [60], enhanced the antifungal effect and enabled reductions above 2.41 $\log_{10}$ steps. This indicates that barrier properties of the fungal cell envelope and the skin matrix can limit PDI and that formulation strategies may be required to unlock full photodynamic potential in topical applications. Formulating PS to enable better drug delivery can optimise PDI efficiency and enable smooth application onto target tissue [61,62]. These findings highlight that performance in homogeneous suspension such as planktonic culture experiments cannot be directly extrapolated to complex tissue or food systems.

Earlier work with curcumin–cyclodextrin systems has largely focused on improving solubility and phototoxicity in homogeneous suspensions or specialised wound dressings, or films for food packaging [58,63]. However, it typically included preparation of nanoparticles or cellulose matrices and targeted standard bacteria [50,59]. In contrast, the present study applies a single, formulation of CD-Cur across multiple matrices, including planktonic cultures, foodstuffs, food-contact surfaces and a porcine skin model. Nonetheless, some limitations of this study must be acknowledged. The experiments were mainly performed using a narrow-band blue LED lamp (435 nm $\pm$ 10 nm) at relatively high radiant exposures. Notably, the experiments performed on plastic foil provided indications of a potential transition toward white-light illumination. This finding may suggest the feasibility of replacing specialised illumination sources with ambient white light, potentially reducing associated illumination costs. Future studies must therefore include a comparison of activation of CD-Cur by blue versus broad-band white light. Photobleaching was visible

after illumination in several matrices, which was confirmed by reduced absorbance of the substance during bleaching (Figure 1B). While this supports antimicrobial action, it may also limit repeated or prolonged use of CD-Cur.

Given the limited number of biological replicates and the substantial log reductions observed, no inferential statistical analyses, including hypothesis testing, multiple-comparison correction, effect-size estimates, confidence intervals, or *p*-values were performed here. This study should therefore be regarded as an initial proof-of-concept. The pronounced reductions observed need confirmation in follow-up studies with a larger number of independent biological replicates. Another limitation of this study is that the characterisation was restricted to functional photophysical and antimicrobial properties. Complementary structural and morphological analyses were not performed and could provide further insight into the characteristics of the investigated system in future studies.

The rapid bleaching of the substances could potentially be exploited as a colour indicator for assessing treatment efficacy. Future studies should investigate how bleaching affects durability and correlates with microbe toxicity. The selected model systems may not fully reflect contamination across the tested matrices. Future studies should therefore extend CD-Cur-based PDI to biofilm and food-processing models, while optimising light delivery and formulations and systematically assessing sensory and safety aspects in food and skin applications. Still, this study presents a proof-of-concept supporting the idea of "One Health, One Photosensitiser", demonstrating that one core CD-Cur formulation, with only minor adjustments in concentration or delivery vehicle (e.g., hydrogel), can simplify PDI of both Gram-negative bacterial and yeast pathogens in diverse, application-relevant environments.

4. Materials and Methods

4.1. CD-Cur Preparation, Characterisation and Stock Solution

A curcuminoid (curcumin, Product Nr. 9469.1, Carl Roth GmbH + Co., Karlsruhe, Germany) hydroxypropyl-γ-cyclodextrin (HP-γ-CD, Product Nr. 826763, W8 HP Ashland Pharma, Schaffhausen, Switzerland) CD-Cur complex was obtained from PLANTA Naturstoffe Vertriebs GmbH, Vienna, Austria. The preparation method for the complex is currently undergoing patent review. The maximal solubility in ddH_2O was tested by visual inspection compared to native curcumin.

The curcuminoid content was determined by high-performance liquid chromatography (HPLC, L-6200A Pump, L-4250 UV-Vis Detector, Merck Hitachi, Tokyo, Japan) using a Lichrosphere RP-C18 column (250 × 4.6 mm, 5 µm particle size). The analysis was performed under isocratic conditions with a mobile phase consisting of acetonitrile and water at a ratio of 50:50 (*v*/*v*), supplemented with 0.1% phosphoric acid (H_3PO_4, 85%). The mobile phase was delivered at a flow rate of 1.2 mL/min, and the injection volume was 20 µL. Detection was performed using a UV–Vis detector (Hitachi U-2001, Hitachi Ltd., Tokyo, Japan) at a wavelength of 435 nm.

For microbiological assays, the CD-Cur (curcumin weight percentage of 7% (*w*/*w*)) was prepared in sterile DPBS at a concentration of 10 mM. Aliquots of the stock solution were stored frozen in the dark at –20 °C and thawed upon use. Absorption spectra of 100 µM native curcumin in DMSO and 100 µM CD-Cur in Dulbecco's phosphate-buffered saline (DPBS, Sigma Life Science, St. Louis, MO, USA) in the visible light range were measured using an Infinite M200 (Tecan Austria GmbH, Grödig, Austria) microplate reader. Bleaching of native curcumin in DMSO, CD-Cur in DPBS and CD-Cur in hydroxyethyl cellulose (HEC; Carl Roth GmbH + Co., Karlsruhe, Germany) hydrogel were measured after bleaching samples with 435 nm LED light (LED 435-12-30, Roithner Lasertechnik, Vienna, Austria) with 0, 7.5, 25, 50, 75, 100 and 200 J/cm^2 and detecting absorption at

423 nm (Infinite M200, Tecan Austria GmbH, Grödig, Austria). Values were normalised to initial absorption before bleaching. The half-life of bleaching ($t50$) was defined as the radiant exposure required for the normalised absorbance to decrease to 0.50. A linear interpolation was applied between the two consecutive measured absorbances (A1 and A2) at two measured timepoints ($t1$ and $t2$) that bracketed this threshold (Equation (1)).

$$\text{half} - \text{life}(t50) = t1 + \frac{\text{A1} - 0.5}{\text{A1} - \text{A2}}(t2 - t1) \quad (1)$$

4.2. Microorganisms

The Gram-negative pathogens *Escherichia coli* ATCC 25922 (DSM 1103) and *Salmonella enterica* spp. *enterica* (DSM 17058), as well as the yeast *Candidozyma auris* (DSM 21092) were obtained from the Leibnitz Institute, DSMZ-German Collection of Microorganisms and Cell Cultures GmbH, Braunschweig, Germany. The non-pathogenic *E. coli* strain K12 blue-xl1 (Agilent Technologies, previously Stratagene, Santa Clara, CA 95051, USA) was kindly provided by Elena Voglas, University of Salzburg.

Bacteria (*E. coli* and *S. enterica*) were cultivated in Tryptic Soy Broth (TSB, 30 g/L CASO Bouillon, Carl Roth GmbH + Co., Karlsruhe, Germany) and the yeast *C. auris* was cultivated in Potato Glucose Broth (PG, 26.5 g/L, Carl Roth GmbH + Co., Karlsruhe, Germany). Before each experiment a fresh culture was prepared by adding 100 µL microbial culture into 20 mL respective medium at 37 °C. Under constant agitation at 200 rpm, *Salmonella enterica* and *C. auris* were cultivated overnight, while *E. coli* was cultivated for 2 h. Before each experiment, the cultures were at an OD_{600nm} of approximately 0.1. After a PDI experiment, the microorganisms were cultivated on plates of the respective media including 15 g/L of agar (Agar-Agar, Kobe I, Carl Roth GmbH + Co., Karlsruhe, Germany) and cultivated at 37 °C for 24 h (*E. coli*, *S. enterica*) or 48 h (*C. auris*) in a sturdy incubator.

4.3. Illumination Set-Ups

Illumination of planktonic experiments, as well as experiments on abiotic surfaces, foodstuff and porcine skin were done using an array consisting of 480 LEDs with a main wavelength of 435 nm (LED 435-12-30, Roithner Lasertechnik, Vienna, Austria). Experiments on plastic food-wrapping foil were performed using a white-light lamp (SANSI Plant-Growing Lamp, ISC Lightning Direct, SANSI LED Lightning, INC., Union City, CA, USA). Emission spectra of both lamps were measured using a handheld spectrometer (LI-COR® LI-180, LI-COR Bioscience, Lincoln, NE, USA) and are given in Figure S1.

Before each experiment the mean irradiance of the lamps was measured using the LI-COR Li-180 spectrometer and the time of illumination was calculated for reaching the specific radiant exposure (Equation (2)).

$$\textit{illumination time}(\text{s}) = \frac{\textit{radiant exposure } (\text{J/cm}^2)}{\textit{irradiance } (\text{W/cm}^2)} \quad (2)$$

4.4. Photodynamic Inactivation on Planktonic Cultures

The cell cultures were prepared as described in Section 4.2. Experiments were performed as previously described [20,64]. Briefly, for each sample, 1.8 mL aliquots of microbial cell culture were centrifuged for 3 min (830 rcf, 25 °C). The supernatant was aspirated, and the cell pellet was resuspended in 1.8 mL of the respective PS concentration or control solution. Controls included: (i) a double-negative control (no PS, no illumination) containing only DPBS, which serves also as the base line for calculations, (ii) a dark control (highest concentration of CD-Cur, no illumination), and (iii) a light control (no PS, illumination

at the maximal radiant exposure) in DPBS. All PS-related steps were performed in the subdued light to prevent photobleaching.

Samples were transferred in technical triplicates (500 µL each) into a 24-well plate. The double-negative and dark controls were placed in a separate, light-protected plate. Incubation in the dark with the PS (drug-to-light interval, DLI) was either absent (0 min) or done for 15 min. Illumination was performed from below, therefore the plate was fastened on an orbital shaker and above the 435 nm LED array using a clamp attached to the shaker. Post-illumination, technical triplicate samples were pooled (60 µL each) into a single well of a 96-well plate after thorough resuspension. Serial dilutions up to 10^7 were prepared and subsequently plated onto TSB or PG agar. After an incubation of 24 h (bacterial samples) or 48 h (*C. auris*), the colony-forming units (CFUs) were counted.

4.5. Photodynamic Inactivation on Different Matrices

To assess the PDI efficiency of CD-Cur across different matrices, experiments were carried out on surfaces selected according to characteristic habitats of each strain.

4.5.1. Photodynamic Inactivation of *Escherichia coli* K12 on Plastic Foil

Commercial cucumber-wrapping plastic foil was cut into 1.5 × 1.5 cm patches (previously disinfected with 70% (*v*/*v*) ethanol) and placed on Petri dishes. CD-Cur was dissolved in 70% (*v*/*v*) ethanol at concentrations of 0, 30, 50, and 100 µM. This solvent system, containing a defined fraction of ethanol, was selected to minimise PS aggregation and to allow a uniform evaporation and a homogeneous coating to form on the plastic surface. Two hundred microlitres of CD-Cur solution was deposited onto each patch, and the solvent was allowed to evaporate at room temperature in the dark until dry, yielding a visibly uniform coating. *Escherichia coli* K-12 was grown to exponential phase (OD600 ≈ 0.4–0.6) in TSB, then centrifuged and resuspended in DPBS. Twenty microlitres of the *E. coli* K12 suspension were inoculated onto each Petri dish and covered with plastic foil coated with CD-Cur. Samples were illuminated from above with a broad-spectrum white-light source delivering a total radiant exposure of 100 J/cm^2 (SANSI Plant-Growing Lamp, ISC Lightning Direct, SANSI LED Lightning, Inc., Union City, CA, USA, at 355 W/m^2). Corresponding dark controls were protected from light and otherwise handled identically. Negative controls (no PS, no illumination) and PS-only controls (100 µM PS, no illumination) and a light control (no PS with illumination) were included.

After treatment, bacteria were recovered by washing each patch with 500 µL DPBS using gentle pipette agitation; the wash was collected. Serial dilutions were prepared, appropriate dilutions were plated on TSB agar plates, samples were incubated for 24 h (37 °C), and colony-forming units (CFU) were counted.

4.5.2. Photodynamic Inactivation of *Escherichia coli* on Abiotic Surfaces

The disinfection properties of CD-Cur against a pathogenic *E coli* strain were tested on three different abiotic surface types: (i) ceramics (plate), (ii) plastic (poly(methyl methacrylate), acrylic) and (iii) metal (stainless steel). All materials were obtained in a local hardware store. Surfaces were cleaned with water and dish soap, then decontaminated before experiments by exposure to 70% (*v*/*v*) ethanol for 3 min and wiped dry.

Twenty microliters of a 2 h bacterial culture were pipetted onto each surface and allowed to dry completely (approximately 1 h). Seventy-five microliters of CD-Cur in DPBS were added to the inoculated spots at concentrations of 30 µM, 50 µM, or 100 µM. Controls included a negative control (no PS, no illumination), a dark control (100 µM CD-Cur without illumination), and a light control (no PS with illumination). Surfaces were illuminated from above with the LED array (435 nm, 25 J/cm^2). Cells were recovered after illumination by swabbing the surface for approximately 1 min with a moist cotton stick,

transferring the swab into an Eppendorf tube containing 450 µL DPBS, and mixing for ~30 s. Samples were serially diluted up to a dilution factor of 10^7 and plated onto TSB agar plates. Plates were incubated overnight at 37 °C, and CFUs were counted.

4.5.3. Photodynamic Inactivation of *Salmonella enterica* on Foodstuff

Salmon skin was cut into approximately 2 × 2 cm sections and placed in 12-well plates. To reduce background contamination, samples were pre-treated with diluted sodium hypochlorite solution (Carl Roth GmbH + Co., Karlsruhe, Germany) applied using sterile cotton swabs. After 1 min, samples were rinsed twice with sterile water and dried under sterile conditions in a laminar flow hood. Each sample was inoculated with 20 µL of a *S. enterica* overnight culture. Subsequently, 100 µL of CD-Cur solutions at concentrations of 30, 50, or 100 µM were added to the respective wells. The experimental design included an untreated double-negative control, receiving DPBS only without illumination or PS, a light control, receiving DPBS and illumination only, and a dark control, treated with 100 µM CD-Cur but without illumination. Samples were incubated in the dark under sterile conditions for a DLI of 15 min. For illumination, samples were exposed to blue light at 435 nm using 100 or 200 J/cm^2. After illumination, 500 µL of DPBS was added to each salmon skin sample, and bacteria were detached by repeated pipetting. Samples were serially diluted and plated onto TSB agar plates. Plates were incubated overnight at 37 °C, and CFUs were counted.

Experiments on pistachios were performed following the protocol described for salmon skin with minor alterations. For that, halved pistachios were inoculated with 20 µL *S. enterica* overnight culture and kept in the laminar air flow to dry for 30 min, before the addition of PS solution. PDI treatment, illumination, serial dilution, and CFU enumeration were then carried out as described above.

To assess whether illumination with the 435 nm LED array caused relevant heating during treatment, the surface temperature of pistachios and salmon skin samples was measured every 30 min during illumination up to a total radiant exposure of 300 J/cm^2. Measurements were performed using a digital thermometer. Two independent experiments were conducted for each sample type.

4.5.4. Photodynamic Inactivation of *Candidozyma auris* on a Porcine Skin Model

To test whether the novel CD-Cur complex has also a potential medical application on skin, a porcine skin model was adapted [65]. Porcine skin (*Sus scrofa domestica*) was obtained from a local butcher, washed with ddH_2O, disinfected with 70% (*v*/*v*) ethanol, and stored at –20 °C until use. Frozen skin was cut into round 1.5 cm diameter pieces using a hole punch and embedded in 1 mL agarose (15 g/L) in 12-well plates. After solidification, samples were disinfected with 70% ethanol for 3 min before use.

As an alternative delivery vehicle for the PS to the porcine skin, a 1% (*w*/*v*) hydroxyethyl cellulose (HEC; Carl Roth GmbH + Co., Karlsruhe, Germany) hydrogel was prepared. Therefore, 0.5 g HEC were added to 50 mL Millipore water (atrium® pro UV; Sartorius AG, Göttingen, Germany) in a 100 mL glass flask and stirred on a heating plate at < 50 °C until the solution became clear and the powder was fully dissolved. The hydrogel was stored at 4 °C until use.

To test whether enhancing cell wall permeability of *C. auris* would increase the PDI effect of CD-Cur, some samples were spiked with 2 mM ethylenediaminetetraacetic acid disodium salt (EDTA; 372.24 g/mol; VWR International, Leuven, Belgium). Therefore, a stock of 400 mM was prepared in Millipore water and stored at room temperature upon use.

For inoculation, *C. auris* overnight cultures were centrifuged, and the pellet was re-suspended in DPBS. Ten microliters of the cell suspension were applied to each skin

sample and allowed to dry under laminar flow. Subsequently, 75 µL of CD-Cur in 1% (*w*/*v*) HEC hydrogel were applied to the skin and distributed evenly with a micro-pestle. Final CD-Cur concentrations of 100 µM and 500 µM were tested. Controls included a dark control (100 µM PS, no illumination), a light control (no PS, illumination), and a no-treatment control (no PS, no illumination). Samples were incubated in the dark for 15 min, followed by illumination with the LED array (435 nm, 75 J/cm^2). Dark controls were kept protected from light. After treatment, yeast cells were recovered by swabbing the skin surface with sterile moistened swabs by scrubbing for 1 min, transferring the swabs to DPBS, and mixing for 30 s. The recovered suspension was serially diluted, plated on PG agar, incubated for 48 h at 37 °C, and CFUs were enumerated.

4.6. Data Evaluation

The photoantimicrobial effect of CD-Cur was assessed using relative inactivation as determined in Equation (3).

$$\text{relative inactivation} = \frac{\text{CFU/mL}_{\text{double negative control}}}{\text{CFU/mL}_{\text{sample}}} \quad (3)$$

All experiments were carried out at least in three biological replicates ($n \geq 3$) in three independent experiments at different timepoints. Exact numbers of replicates are given in the Supplementary Materials for each set of experiments. Relative inactivation was calculated for each biological replicate and results were combined to calculate the mean relative inactivation. Standard deviations were calculated for all conditions, and data were visualised using MATLAB (Version 2024b, The MathWorks, Inc, Portola Valley, CA, USA).

To compare treatment efficacy, all graphs include a threshold line at 3 $\log_{10}$ reduction, corresponding to a 99.9% decrease in viable cells. This threshold is widely accepted in microbiology as the minimum level for an antimicrobial effect and for evaluating treatment potency [56].

5. Conclusions

This study provides proof-of-concept that a single, food-grade curcumin-based PS can effectively inactivate main One Health-relevant pathogens across diverse matrices, including planktonic cultures, abiotic surfaces, foodstuff and a porcine skin model. CD-Cur demonstrates concentration-dependent photoinactivation, exceeding 99.9% cell killing, in liquid culture and on selected surfaces. Biologically relevant inactivation has been shown on salmon and pistachios without visible colour alteration and enhanced antifungal activity against *C. auris* in a hydrogel formulation. With this highly diverse approach we could give a first hint that food-grade CD-Cur, activated by visible blue light, could be a promising PS within the One Health scope. Especially, the food-production chain could profit from this straightforward, inexpensive but effective system. CD-Cur-based PDI thus represents a promising tool to strengthen microbial safety in food processing and explore adjunctive applications in skin disinfection and healthcare settings.

Supplementary Materials: The following supporting information can be downloaded at https://www.mdpi.com/article/10.3390/antibiotics15111049/s1, Figure S1: Emission spectra of used lamps; Figure S2. Mean relative inactivation of *Salmonella enterica* at increased DLI; Figure S3. *Salmonella enterica* decontamination on foodstuff at 100 J/cm2; Table S1. Results overview of liquid culture experiments; Table S2. Results overview of PDI of *Escherichia coli* on plastic foil; Table S3. Results light toxicity evaluation (435 nm at different radiant exposures) of *Escherichia coli*; Table S4. Results overview of PDI of *Escherichia coli* on various abiotic surfaces; Table S5. Temperatures measured on pistachio and salmon skin samples upon exposure to the 435 nm LED array;

Table S6. Results overview of PDI of *Salmonella enterica* on different foodstuffs; Table S7. Preliminary experiments of PDI of *Candidozyma auris* on porcine skin using different concentrations of CD-Cur without the addition of 1% HEC; Table S8. Results overview of PDI of *Candidozyma auris* on t

Author Contributions: Conceptualization, A.K., K.P., L.J. and L.W.; methodology, A.C., A.K., E.F. and I.S.; analysis, A.C., A.K., E.F., I.S. and L.J.; investigation, A.C., A.K., E.F., I.S. and L.J.; resources, K.P. and L.W.; data curation, A.K., K.P. and L.J.; writing—original draft preparation, A.C., A.K., E.F., I.S. and L.J.; writing—review and editing, A.C., A.K., E.F., I.S., K.P., L.J. and L.W.; visualisation, L.J.; supervision, K.P. and L.J.; project administration, L.J. and K.P.; funding acquisition, K.P. All authors have read and agreed to the published version of the manuscript.

Funding: This research received no external funding.

Institutional Review Board Statement: Not applicable.

Informed Consent Statement: Not applicable.

Data Availability Statement: The original contributions presented in this study are included in the article/Supplementary Materials. Further inquiries can be directed to the corresponding author.

Acknowledgments: The authors are grateful to Elena Voglas, University of Salzburg for providing *Escherichia coli* K12 and to PLANTA Naturstoffe Vertriebs GmbH, Vienna, Austria for providing CD-Cur. Artificial intelligence (AI) tools (Perplexity AI, basic plan version) were used solely for English language editing, including grammar correction, proofreading, and linguistic refinement. No AI tools were used to generate scientific content, interpret results, or draw conclusions. The authors have reviewed and edited the output and take full responsibility for the content of this publication.

Conflicts of Interest: A.K. and L.W. are shareholders and management team at PLANTA Naturstoffe Vertriebs GmbH; however, they participated in this study solely in the capacity of scientists and research assistants. The remaining authors declare that the research was conducted in the absence of any commercial or financial relationships that could be construed as a potential conflict of interest.

Abbreviations

The following abbreviations are used in this manuscript:

CD-Cur	curcuminoid complexed with hydroxypropyl-γ-cyclodextrin
DLI	drug to light interval
DMSO	dimethyl sulfoxide
DPBS	Dulbecco's phosphate-buffered saline
EDTA	ethylenediaminetetraacetic acid disodium salt
HEC	hydroxyethyl cellulose
HPLC	high-performance liquid chromatography
HP-γ-CD	hydroxypropyl-γ-cyclodextrin
OD600	optical density at 600 nm
PDI	Photodynamic Inactivation
PG	potato glucose broth
PS	photosensitiser
ROS	reactive oxygen species
TSB	tryptic soy broth

References

1. Destoumieux-Garzón, D.; Mavingui, P.; Boetsch, G.; Boissier, J.; Darriet, F.; Duboz, P.; Fritsch, C.; Giraudoux, P.; Le Roux, F.; Morand, S.; et al. The One Health Concept: 10 Years Old and a Long Road Ahead. *Front. Vet. Sci.* **2018**, *5*, 14. [CrossRef]
2. Boqvist, S.; Söderqvist, K.; Vågsholm, I. Food safety challenges and One Health within Europe. *Acta Vet. Scand.* **2018**, *60*, 1. [CrossRef]
3. Garcia, S.N.; Osburn, B.I.; Jay-Russell, M.T. One Health for Food Safety, Food Security, and Sustainable Food Production. *Front. Sustain. Food Syst.* **2020**, *4*, 1. [CrossRef]

4. Barcenilla, C.; Cobo-Díaz, J.F.; Puente, A.; Valentino, V.; De Filippis, F.; Ercolini, D.; Carlino, N.; Pinto, F.; Segata, N.; Prieto, M.; et al. In-depth characterization of food and environmental microbiomes across different meat processing plants. *Microbiome* **2024**, *12*, 199. [CrossRef]
5. Maes, S.; Heyndrickx, M.; Vackier, T.; Steenackers, H.; Verplaetse, A.; Reu, K.D. Identification and Spoilage Potential of the Remaining Dominant Microbiota on Food Contact Surfaces after Cleaning and Disinfection in Different Food Industries. *J. Food Prot.* **2019**, *82*, 262–275. [CrossRef]
6. Lake, R.J.; Devleesschauwer, B.; Majowicz, S.E.; Robertson, L.J.; Jakobsen, L.S.; Agudo, A.; Pires, S.M.; Kirk, M.D.; Walter, E.S.; Keddy, K.H.; et al. WHO estimates of the global, regional, and national burden of 42 foodborne infectious and chemical hazards, 2000–21: An updated data synthesis. *Lancet Glob. Health* **2026**, *14*, 103994. [CrossRef]
7. Miller, M.A.; Sentz, J.; Rabaa, M.A.; Mintz, E.D. Global epidemiology of infections due to Shigella, Salmonella serotype Typhi, and enterotoxigenic Escherichia coli. *Epidemiol. Infect.* **2008**, *136*, 433–435. [CrossRef]
8. Arora, P.; Singh, P.; Wang, Y.; Yadav, A.; Pawar, K.; Singh, A.; Padmavati, G.; Xu, J.; Chowdhary, A. Environmental Isolation of Candida auris from the Coastal Wetlands of Andaman Islands, India. *mBio* **2021**, *12*, e03181-20. [CrossRef]
9. Omardien, S.; Teska, P. Skin and hard surface disinfection against Candida auris—What we know today. *Front. Med.* **2024**, *11*, 1312929. [CrossRef]
10. Yadav, A.; Jain, K.; Wang, Y.; Pawar, K.; Kaur, H.; Sharma, K.K.; Tripathy, V.; Singh, A.; Xu, J.; Chowdhary, A. Candida auris on Apples: Diversity and Clinical Significance. *mBio* **2022**, *13*, e00518-22. [CrossRef]
11. Roth, N.; Käsbohrer, A.; Mayrhofer, S.; Zitz, U.; Hofacre, C.; Domig, K.J. The application of antibiotics in broiler production and the resulting antibiotic resistance in *Escherichia coli*: A global overview. *Poult. Sci.* **2019**, *98*, 1791–1804. [CrossRef]
12. Rushton, J.; Ferreira, J.P.; Stärk, K.D.C. Antimicrobial Resistance: The Use of Antimicrobials in the Livestock Sector. *OECD Food, Agriculture and Fisheries Papers*, 9 October 2014. [CrossRef]
13. Carrasco, E.; Morales-Rueda, A.; García-Gimeno, R.M. Cross-contamination and recontamination by *Salmonella* in foods: A review. *Food Res. Int.* **2012**, *45*, 545–556. [CrossRef]
14. Marshall, K.E.; Hexemer, A.; Seelman, S.L.; Fatica, M.K.; Blessington, T.; Hajmeer, M.; Kisselburgh, H.; Atkinson, R.; Hill, K.; Sharma, D.; et al. Lessons Learned from a Decade of Investigations of Shiga Toxin–Producing Escherichia coli Outbreaks Linked to Leafy Greens, United States and Canada. *Emerg. Infect. Dis.* **2020**, *26*, 2319–2328. [CrossRef]
15. Possas, A.; Pérez-Rodríguez, F. New insights into cross-contamination of fresh-produce. *Curr. Opin. Food Sci.* **2023**, *49*, 100954. [CrossRef]
16. Wainwright, M.; Maisch, T.; Nonell, S.; Plaetzer, K.; Almeida, A.; Tegos, G.P.; Hamblin, M.R. Photoantimicrobials—Are we afraid of the light? *Lancet Infect. Dis.* **2017**, *17*, e49–e55. [CrossRef]
17. Cieplik, F.; Deng, D.; Crielaard, W.; Buchalla, W.; Hellwig, E.; Al-Ahmad, A.; Maisch, T. Antimicrobial photodynamic therapy—What we know and what we don't. *Crit. Rev. Microbiol.* **2018**, *44*, 571–589. [CrossRef]
18. Hamblin, M.R. Antimicrobial photodynamic inactivation: A bright new technique to kill resistant microbes. *Curr. Opin. Microbiol.* **2016**, *33*, 67–73. [CrossRef]
19. Maisch, T.; Hackbarth, S.; Regensburger, J.; Felgenträger, A.; Bäumler, W.; Landthaler, M.; Röder, B. Photodynamic inactivation of multi-resistant bacteria (PIB)—A new approach to treat superficial infections in the 21st century. *JDDG J. Dtsch. Dermatol. Ges.* **2011**, *9*, 360–366. [CrossRef]
20. Wimmer, A.; Glueck, M.; Ckurshumova, W.; Liu, J.; Fefer, M.; Plaetzer, K. Breaking the Rebellion: Photodynamic Inactivation against Erwinia amylovora Resistant to Streptomycin. *Antibiotics* **2022**, *11*, 544. [CrossRef]
21. Cenit, A.; Liu, J.; Fefer, M.; Plaetzer, K. Photodynamic Decontamination of Food: Assessing Surface Challenges Against Listeria monocytogenes. *Microorganisms* **2026**, *14*, 59. [CrossRef]
22. Fellner, A.; Hamminger, C.; Fefer, M.; Liu, J.; Plaetzer, K. Towards Microbial Food Safety of Sprouts: Photodynamic Decontamination of Seeds. *Photonics* **2023**, *10*, 239. [CrossRef]
23. Ruan, S.; Zhu, T.; Zuo, C.; Peng, J.; Liu, L.; Lan, W.; Pan, L.; Tu, K. Storage Properties and Shelf-Life Prediction of Fresh-Cut Radishes Treated by Photodynamic Technology. *Foods* **2024**, *13*, 2367. [CrossRef]
24. Tortik, N.; Spaeth, A.; Plaetzer, K. Photodynamic decontamination of foodstuff from Staphylococcus aureus based on novel formulations of curcumin. *Photochem. Photobiol. Sci.* **2014**, *13*, 1402–1409. [CrossRef]
25. Wang, D.; Kyere, E.; Ahmed Sadiq, F. New Trends in Photodynamic Inactivation (PDI) Combating Biofilms in the Food Industry—A Review. *Foods* **2021**, *10*, 2587. [CrossRef]
26. do Prado-Silva, L.; Brancini, G.T.P.; Braga, G.Ú.L.; Liao, X.; Ding, T.; Sant'Ana, A.S. Antimicrobial photodynamic treatment (aPDT) as an innovative technology to control spoilage and pathogenic microorganisms in agri-food products: An updated review. *Food Control* **2022**, *132*, 108527. [CrossRef]
27. Glueck, M.; Schamberger, B.; Eckl, P.; Plaetzer, K. New horizons in microbiological food safety: Photodynamic Decontamination based on a curcumin derivative. *Photochem. Photobiol. Sci.* **2017**, *16*, 1784–1791. [CrossRef]

28. Prasad, A.; Wynands, E.; Roche, S.M.; Romo-Bernal, C.; Allan, N.; Olson, M.; Levengood, S.; Andersen, R.; Loebel, N.; Sabino, C.P.; et al. Photodynamic Inactivation of Foodborne Bacteria: Screening of 32 Potential Photosensitizers. *Foods* **2024**, *13*, 453. [CrossRef]
29. Winter, S.; Tortik, N.; Kubin, A.; Krammer, B.; Plaetzer, K. Back to the roots: Photodynamic inactivation of bacteria based on water-soluble curcumin bound to polyvinylpyrrolidone as a photosensitizer. *Photochem. Photobiol. Sci.* **2013**, *12*, 1795–1802. [CrossRef]
30. Food and Feed Information Portal Database EC. Curcumin | Food and Feed Information Portal Database | FIP. 2026. Available online: https://ec.europa.eu/food/food-feed-portal/screen/food-additives/search/details/POL-FAD-IMPORT-2985 (accessed on 15 July 2026).
31. Nelson, K.M.; Dahlin, J.L.; Bisson, J.; Graham, J.; Pauli, G.F.; Walters, M.A. The Essential Medicinal Chemistry of Curcumin: Miniperspective. *J. Med. Chem.* **2017**, *60*, 1620–1637. [CrossRef]
32. Hussain, Y.; Alam, W.; Ullah, H.; Dacrema, M.; Daglia, M.; Khan, H.; Arciola, C.R. Antimicrobial Potential of Curcumin: Therapeutic Potential and Challenges to Clinical Applications. *Antibiotics* **2022**, *11*, 322. [CrossRef]
33. Yang, X.; Palasuberniam, P.; Kraus, D.; Chen, B. Aminolevulinic Acid-Based Tumor Detection and Therapy: Molecular Mechanisms and Strategies for Enhancement. *Int. J. Mol. Sci.* **2015**, *16*, 25865–25880. [CrossRef]
34. Dobson, J.; de Queiroz, G.F.; Golding, J.P. Photodynamic therapy and diagnosis: Principles and comparative aspects. *Vet. J.* **2018**, *233*, 8–18. [CrossRef]
35. Kwiatkowski, S.; Knap, B.; Przystupski, D.; Saczko, J.; Kędzierska, E.; Knap-Czop, K.; Kotlińska, J.; Michel, O.; Kotowski, K.; Kulbacka, J. Photodynamic therapy—Mechanisms, photosensitizers and combinations. *Biomed. Pharmacother.* **2018**, *106*, 1098–1107. [CrossRef]
36. Xie, L.; Ji, X.; Zhang, Q.; Wei, Y. Curcumin combined with photodynamic therapy, promising therapies for the treatment of cancer. *Biomed. Pharmacother.* **2022**, *146*, 112567. [CrossRef]
37. Santezi, C.; Reina, B.D.; Dovigo, L.N. Curcumin-mediated Photodynamic Therapy for the treatment of oral infections—A review. *Photodiagnosis Photodyn. Ther.* **2018**, *21*, 409–415. [CrossRef]
38. Alven, S.; Nqoro, X.; Aderibigbe, B.A. Polymer-Based Materials Loaded with Curcumin for Wound Healing Applications. *Polymers* **2020**, *12*, 2286. [CrossRef]
39. Vollono, L.; Falconi, M.; Gaziano, R.; Iacovelli, F.; Dika, E.; Terracciano, C.; Bianchi, L.; Campione, E. Potential of Curcumin in Skin Disorders. *Nutrients* **2019**, *11*, 2169. [CrossRef]
40. Nicolaescu, O.E.; Belu, I.; Mocanu, A.G.; Manda, V.C.; Rău, G.; Pîrvu, A.S.; Ionescu, C.; Ciulu-Costinescu, F.; Popescu, M.; Ciocîlteu, M.V. Cyclodextrins: Enhancing Drug Delivery, Solubility and Bioavailability for Modern Therapeutics. *Pharmaceutics* **2025**, *17*, 288. [CrossRef]
41. Shahriari, M.; Kesharwani, P.; Johnston, T.P.; Sahebkar, A. Anticancer potential of curcumin-cyclodextrin complexes and their pharmacokinetic properties. *Int. J. Pharm.* **2023**, *631*, 122474. [CrossRef]
42. Yallapu, M.M.; Jaggi, M.; Chauhan, S.C. β-Cyclodextrin-curcumin self-assembly enhances curcumin delivery in prostate cancer cells. *Colloids Surf. B Biointerfaces* **2010**, *79*, 113–125. [CrossRef]
43. Food and Feed Information Portal Database EC. Cyclodextrin | Food and Feed Information Portal Database | FIP. 2026. Available online: https://ec.europa.eu/food/food-feed-portal/screen/food-additives/search/details/POL-FAD-IMPORT-3164 (accessed on 15 July 2026).
44. Sevim, S.; Sanlier, N. Cyclodextrin as a singular oligosaccharide: Recent advances of health benefit and in food applications. *J. Food Sci.* **2024**, *89*, 8215–8230. [CrossRef]
45. Luksiene, Z. LED-Based Photosensitization—A Prospect for Visible Light-Driven Nonthermal Fresh Produce Sanitation. In *Nonthermal Processing in Agri-Food-Bio Sciences: Sustainability and Future Goals*; Režek Jambrak, A., Ed.; Springer International Publishing: Cham, Swizerland, 2022; pp. 409–445.
46. Damyeh, M.S.; Mereddy, R.; Netzel, M.E.; Sultanbawa, Y. An insight into curcumin-based photosensitization as a promising and green food preservation technology. *Compr. Rev. Food Sci. Food Saf.* **2020**, *19*, 1727–1759. [CrossRef]
47. Araújo, N.C.; Fontana, C.R.; Bagnato, V.S.; Gerbi, M.E.M. Photodynamic antimicrobial therapy of curcumin in biofilms and carious dentine. *Lasers Med. Sci.* **2014**, *29*, 629–635. [CrossRef]
48. Ribeiro, I.d.P.; Pinto, J.G.; Souza, B.M.N.; Miñán, A.G.; Ferreira-Strixino, J. Antimicrobial photodynamic therapy with curcumin on methicillin-resistant *Staphylococcus aureus* biofilm. *Photodiagnosis Photodyn. Ther.* **2022**, *37*, 102729. [CrossRef]
49. Spaeth, A.; Graeler, A.; Maisch, T.; Plaetzer, K. CureCuma–cationic curcuminoids with improved properties and enhanced antimicrobial photodynamic activity. *Eur. J. Med. Chem.* **2018**, *159*, 423–440. [CrossRef]
50. Gutierrez, J.K.T.; Zanatta, G.C.; Ortega, A.L.M.; Balastegui, M.I.C.; Sanitá, P.V.; Pavarina, A.C.; Barbugli, P.A.; Mima, E.G.d.O. Encapsulation of curcumin in polymeric nanoparticles for antimicrobial Photodynamic Therapy. *PLoS ONE* **2017**, *12*, e0187418. [CrossRef]
51. Mirzahosseinipour, M.; Khorsandi, K.; Hosseinzadeh, R.; Ghazaeian, M.; Shahidi, F.K. Antimicrobial photodynamic and wound healing activity of curcumin encapsulated in silica nanoparticles. *Photodiagnosis Photodyn. Ther.* **2020**, *29*, 101639. [CrossRef]

52. Metzger, M.; Manhartseder, S.; Krausgruber, L.; Scholze, L.; Fuchs, D.; Wagner, C.; Stainer, M.; Grillari, J.; Kubin, A.; Wightman, L.; et al. The Multifaceted Actions of PVP–Curcumin for Treating Infections. *Int. J. Mol. Sci.* **2024**, *25*, 6140. [CrossRef]
53. Wikene, K.O.; Hegge, A.B.; Bruzell, E.; Tønnesen, H.H. Formulation and characterization of lyophilized curcumin solid dispersions for antimicrobial photodynamic therapy (aPDT): Studies on curcumin and curcuminoids LII. *Drug Dev. Ind. Pharm.* **2015**, *41*, 969–977. [CrossRef]
54. Koca Fındık, B.; Yakavets, I.; Lassalle, H.-P.; Catak, S.; Monari, A. Efficient Delivering of a Photodynamic Therapy Drug into Cellular Membranes Rationalized by Molecular Dynamics. *J. Phys. Chem. B* **2024**, *128*, 11625–11633. [CrossRef]
55. Lai, D.; Zhou, A.; Tan, B.K.; Tang, Y.; Sarah Hamzah, S.; Zhang, Z.; Lin, S.; Hu, J. Preparation and photodynamic bactericidal effects of curcumin-β-cyclodextrin complex. *Food Chem.* **2021**, *361*, 130117. [CrossRef]
56. Pearson, R.D.; Steigbigel, R.T.; Davis, H.T.; Chapman, S.W. Method of reliable determination of minimal lethal antibiotic concentrations. *Antimicrob. Agents Chemother.* **1980**, *18*, 699–708. [CrossRef]
57. Huang, J.; Chen, B.; Zeng, Q.-H.; Liu, Y.; Liu, H.; Zhao, Y.; Wang, J.J. Application of the curcumin-mediated photodynamic inactivation for preserving the storage quality of salmon contaminated with *L. monocytogenes*. *Food Chem.* **2021**, *359*, 129974. [CrossRef]
58. Chen, L.; Dong, Q.; Shi, Q.; Du, Y.; Zeng, Q.; Zhao, Y.; Wang, J.J. Novel 2,3-Dialdehyde Cellulose-Based Films with Photodynamic Inactivation Potency by Incorporating the β-Cyclodextrin/Curcumin Inclusion Complex. *Biomacromolecules* **2021**, *22*, 2790–2801. [CrossRef]
59. Wu, J.; Li, J.; Xu, F.; Zhou, A.; Zeng, S.; Zheng, B.; Lin, S. Effective Preservation of Chilled Pork Using Photodynamic Antibacterial Film Based on Curcumin-β-Cyclodextrin Complex. *Polymers* **2023**, *15*, 1023. [CrossRef]
60. De Nobel, J.G.; Dijkers, C.; Hooijberg, E.; Klis, F.M. Increased Cell Wall Porosity in Saccharomyces cerevisiae after Treatment with Dithiothreitol or EDTA. *Microbiology* **1989**, *135*, 2077–2084. [CrossRef]
61. Maldonado-Carmona, N.; Ouk, T.-S.; Leroy-Lhez, S. Latest trends on photodynamic disinfection of Gram-negative bacteria: Photosensitizer's structure and delivery systems. *Photochem. Photobiol. Sci.* **2022**, *21*, 113–145. [CrossRef]
62. Tim, M. Strategies to optimize photosensitizers for photodynamic inactivation of bacteria. *J. Photochem. Photobiol. B Biol.* **2015**, *150*, 2–10. [CrossRef]
63. Gupta, A.; Briffa, S.M.; Swingler, S.; Gibson, H.; Kannappan, V.; Adamus, G.; Kowalczuk, M.; Martin, C.; Radecka, I. Synthesis of Silver Nanoparticles Using Curcumin-Cyclodextrins Loaded into Bacterial Cellulose-Based Hydrogels for Wound Dressing Applications. *Biomacromolecules* **2020**, *21*, 1802–1811. [CrossRef]
64. Glueck, M.; Hamminger, C.; Fefer, M.; Liu, J.; Plaetzer, K. Save the crop: Photodynamic Inactivation of plant pathogens I: Bacteria. *Photochem. Photobiol. Sci.* **2019**, *18*, 1700–1708. [CrossRef]
65. Tortik, N.; Steinbacher, P.; Maisch, T.; Spaeth, A.; Plaetzer, K. A comparative study on the antibacterial photodynamic efficiency of a curcumin derivative and a formulation on a porcine skin model. *Photochem. Photobiol. Sci.* **2016**, *15*, 187–195. [CrossRef]

Disclaimer/Publisher's Note: The statements, opinions and data contained in all publications are solely those of the individual author(s) and contributor(s) and not of MDPI and/or the editor(s). MDPI and/or the editor(s) disclaim responsibility for any injury to people or property resulting from any ideas, methods, instructions or products referred to in the content.